The Adsorption Dynamics of Molecular Methane, Propane, and Neopentane on Pd(111): Theory and Experiment†

Chia-Ling Kao and Robert J. Madix*

Chemical Engineering Department, Stanford University, Stanford, California 94305

Received: March 13, 2002; In Final Form: June 13, 2002

The molecular adsorption dynamics of methane, propane, and neopentane on Pd(111) was studied using supersonic molecular beam techniques and stochastic trajectory simulations. The sticking probability of the alkanes was measured as a function of incident energy, incident angle, and alkane coverage. In each case, the trapping probability decreased with increasing incident translational energy, which is expected for nonactivated molecular trapping. Nonnormal energy scaling was observed for the trapping probability of all of these alkanes, indicating corrugation of the gas−surface interaction potentials. The modified Kisliuk model was employed to describe the self-coverage dependence of the alkane on Pd(111). The trapping probability of each of these alkanes on Pd(111) is higher than that on Pt(111), consistent with the lower mass of palladium. Using the Morse potential for the methyl (methylene)−platinum two body potential obtained from the stochastic trajectory analyses of alkanes trapping on Pt(111), the trapping probabilities of alkanes on Pd(111) were predicted nearly exactly. Energy transfer calculations for alkane trapping on Pd(111) clearly indicate that excitation of the lattice vibrations and molecular cartwheeling rotations are the principal mechanisms for determining trapping.

1. Introduction

An understanding of adsorption kinetics is important because the adsorption of molecules on bare or partially covered surfaces is the first step in any heterogeneously catalyzed reaction. Furthermore, because of microscopic reversibility, desorption mirrors adsorption, and the understanding of the dynamics of adsorption can yield valuable insights into desorption as well. Because of the importance of platinum group metals as catalysts, many studies of the dynamics of adsorption of weakly interacting gas−surface systems on Pt surfaces have been reported recently.

Schoofs et al.[21] began investigating the trapping of ethane on Pt(111) using direct sticking probability measurements. Arumainayagam et al.[3] found that the initial trapping probability of ethane on Pt(111) decreases with increasing incident kinetic energy and exhibits an energy scaling function of $E_T \cos^{0.6}\theta$, suggesting a corrugated gas−surface potential. Later, the dynamics of propane trapping on Pt(111) was studied by McMaster et al.[18] Similar to ethane, the empirical energy function $E_T \cos^{0.6}\theta$ collapsed the energy and angular dependences of the trapping probability of propane onto one smooth curve. In contrast, methane trapping on Pt(111) exhibits an energy scaling of $E_T \cos^{1.5}\theta$, suggesting a smooth corrugation in the gas−surface potential.[2,4] Subsequently, the dynamics of *n*-butane, isobutane, and neopentane trapping on Pt(111) was studied by Weaver and Madix.[29] Both *n*-butane and isobutane exhibit the energy scaling function of $E_T \cos^{0.8}\theta$. On the other hand, neopentane scaled with $E_T \cos^{1.3}\theta$. The authors attributed the enhanced angular dependence of trapping probability for neopentane to its higher molecular weight.

To better understand the energy transfer process involved in adsorption, realistic molecular simulations of alkane adsorption were under taken by Stinnett et al.[22] for ethane trapping on Pt(111). By using an empirical, pairwise additive Morse potential to represent the ethane−Pt interaction, good agreement between experiments and simulations was obtained. Subsequently, this set of potential parameters was successfully employed to quantitatively predict the molecular adsorption dynamics of ethane on Pt(110)−(1 × 2),[24] Pt(111)−S,[25] and Pt(111)−O.[13] Stinnett et al. also extend their calculations to methane and propane on Pt(111) and Pt(110)−(1 × 2),[23] finding excellent quantitative agreement between experiment and theory for the trapping probability at a wide variety of incident energies and angles. Later, Weaver et al. extended the united-atom approach to model the dynamics of *n*-butane, isobutane, and neopentane on Pt(111) using the same simulation methods[29] and successfully reproduced the angular and energy dependencies on incident energy and angle. In the latter work, the Morse potential was adjusted slightly to give a better fit of theory and experiment for all of the alkanes, C_1-C_5. For all of the systems investigated, the molecular dynamics provided insights into the energy or momentum exchange processes governing trapping of the alkanes.

Because palladium and platinum are in the same column of the periodic table, the physical properties of the two metals are quite similar. The bond lengths of palladium (2.751 Å) and platinum (2.774 Å) are almost the same,[17] the bulk Debye temperature of palladium (273.4 K) is close to that of platinum (234 K),[10] and the surface Debye temperatures differ rather little ($T_{D,Pd} = 140 \pm 10$ K; $T_{D,Pt} = 110 \pm 10$ K).[10] Furthermore, the desorption temperature of low molecular weight alkanes on palladium are similar to those on platinum (Table 1). The similarity of the desorption temperatures of the two surfaces

† Part of the special issue "John C. Tully Festschrift".
* To whom correspondence should be addressed.

10.1021/jp020706a CCC: $22.00
Published on Web 07/20/2002

TABLE 1: Desorption Temperatures (K) of Alkanes on Pt(111) and Pd(111)

	Pt(111)	Pd(111)		Pt(111)	Pd(111)
methane	64	67	propane	150	162
ethane	115	120	neopentane	200	200

suggests that the potential energy functions between the alkanes and the surfaces may be similar. However, the masses of the two metals are quite different; palladium is about half the atomic weight of platinum (mass Pd = 106.4 g/mol, mass Pt = 195.09 g/mol). Thus, the adsorption dynamics and the adsorption probabilities of alkanes on Pd(111) may be different from those on Pt(111) because of this difference in mass. In other words, the palladium and platinum surfaces offer the opportunity to examine the importance of mass of the surface atoms during adsorption and, because of the similarity in the other dynamical parameters governing the trapping process, to test the predictive capability of the theory to scale trapping probabilities from one metal to another.

Previously, we reported the study of the dynamics of *ethane* trapping on Pd(111), studied experimentally using supersonic molecular beams and theoretically by molecular dynamics simulations.[14] The trapping probability of ethane on Pd(111) is slightly higher than it is on Pt(111), consistent with the lower mass of palladium. The energy scalings for both surfaces are nearly the same, suggesting a similar degree of corrugation on the gas−surface potentials. Calculations of the energy transfer for ethane after the first bounce on Pd(111) clearly indicate that vibrational excitation of the solid accounts primarily for the increase in trapping probabilities of ethane on Pd(111) above Pt(111). The enhancement in lattice excitation results from increasing the mass ratio of ethane to the metal atoms.

In this supersonic molecular beam study, the molecular adsorption probabilities of methane, propane, and neopentane on Pd(111) were determined as a function of incident energy and incident angle at temperatures well below their desorption temperatures. The differences of alkanes adsorption on Pt(111) and Pd(111) are compared, and the predictive capabilities of the molecular dynamics approach to predicting adsorption probabilities on different metals are discussed.

2. Experimental Section

The experimental apparatus used in this study has been described in detail elsewhere.[6] Briefly, it consists of an ultrahigh vacuum chamber with a base pressure of 5×10^{-11} Torr coupled to a triply pumped supersonic molecular beam source. The main chamber is equipped with a rear view LEED/AES electron optics and two quadrupole mass spectrometers. One mass spectrometer is mounted on a bellows and is equipped with a collimating cap[8,9] on the ionizer. The second mass spectrometer can be rotated 180° about the sample at a fixed radius of 10.5 cm and is used in conjunction with a lock-in amplifier and 50% duty beam chopper to measure the velocity of the molecules in the beam.

The Pd(111) crystal was cleaned by cycles of Ar^+ sputtering and oxygen cleaning. Because of the limitation of AES to distinguish carbon on the surface from Pd, the temperature-programmed reaction of oxygen on Pd(111) was used to verify the cleanliness of the crystal. When a sharp p(1 × 1) hexagonal LEED pattern was observed and a clean oxygen TPD peak was shown without the presence of CO or CO_2, the surface was assumed to be clean and well ordered. In general, only two cycles of oxygen cleaning were needed at the beginning of each day. In addition, one cycle of oxygen treatment and annealing to 1000 K were performed to ensure surface cleanliness before each measurement.

A tungsten filament mounted behind the crystal provided radiation for heating to 800 K and a source of electrons for heating to 1200 K. Liquid-nitrogen flow through the sample holder allowed the surface to cool to 95 K. For lower temperatures, liquid helium was supplied. Temperatures were measured to ±0.5 K using 0.125 mm chromel−alumel thermocouple wires spot-welded to the back of the crystal. The molecular beam was formed by the supersonic expansion of gas through a monel nozzle that could be heated resistively with proportional-integral-derivative (PID) control to 750 K without clogging the nozzle. A uniform flux of molecules was delivered to the crystal of about 10^{14}/s onto a 0.058 cm^2 spot. Low energy beams were formed with pure gas, whereas high-energy beams were formed by seeding gas in helium and heating the nozzle.

The method of King and Wells[15] was used to measure direct sticking probabilities using a shutter in the beam source chamber and an inert, gold-plated flag in the main chamber. The partial pressure of incoming molecules in the beam was measured with the stationary mass spectrometer as a function of time. When the shutter and flag were both blocking the beam, a background reference was taken. At 20 s, the shutter was opened, and the background pressure due to the beam scattering off the inert flag was measured. At 40 s, the flag was lowered, and the beam was allowed to impinge on the crystal. At our large pumping speeds,[7] the ratio of the drop in the partial pressure measured at time t to the initial partial pressure when it scatters off the inert flag gives the net sticking probability on the surface. Initial trapping probabilities were measured with an experimental error estimated to be ±0.02 for various incident angles and energies.

The crystal was rotated to angles from 0 to 60° to the incident beam for the trapping probability measurements. It was verified that the entire beam was impinging on the crystal at each position by monitoring the absence of a modulated helium beam behind the crystal, using the rotatable mass spectrometer at the back of the chamber. At glancing incident angles, the crystal was turned away from the stationary mass spectrometer to avoid contributions from directly scattered components to the sticking probability measurement.

3. Experimental Results

Figure 1 shows the initial trapping probability of methane on Pd(111) as a function of incident energy and incident angle at the surface temperature of 50 K, well below its desorption temperature of 67 K. As the incident energies are increased from 7.7 to 16.4 kJ/mol and the angle of incidence is varied from 0 to 60°, the initial trapping probability of methane on Pd(111) decreases from 0.8 to 0.05. These data are best scaled by energy scaling function of $E_T \cos^{1.0 \pm 0.1}\theta$.

The initial trapping probability of propane on Pd(111) as a function of incident energy and angle at a surface temperature of 95 K is shown in Figure 2. In the range of the normal incident energies from 11.6 to 56 kJ/mol, the trapping probability of propane decreases from unity to 0.4. The scaling function $E_T \cos^{0.9 \pm 0.1}\theta$ best collapses the energy and angular dependencies onto one curve.

The initial trapping probability of neopentane incident upon Pd(111) is shown as a function of incident energy and incident angle in Figure 3. At a surface temperature of 130 K, the trapping probability of neopentane on Pd(111) decreases from unity to 0.2 in the range of normal incident energy of 15.7 to 113.5 kJ/mol. The best energy scaling function for neopentane trapping on Pd(111) is $E_T \cos^{0.9 \pm 0.1}\theta$.

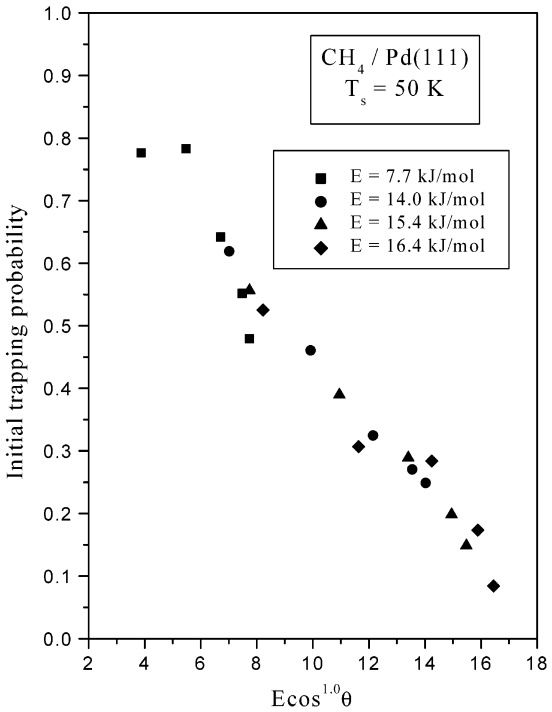

Figure 1. Initial trapping probability of methane on Pd(111) at the surface temperature of 50 K plotted as a function of $E_T \cos^{1.0}\theta$. The incident angle is measured from the surface normal. The incident energies, E_T, are 7.7 (■), 14.0 (●), 15.4 (▲), and 16.4 (♦) kJ/mol, respectively.

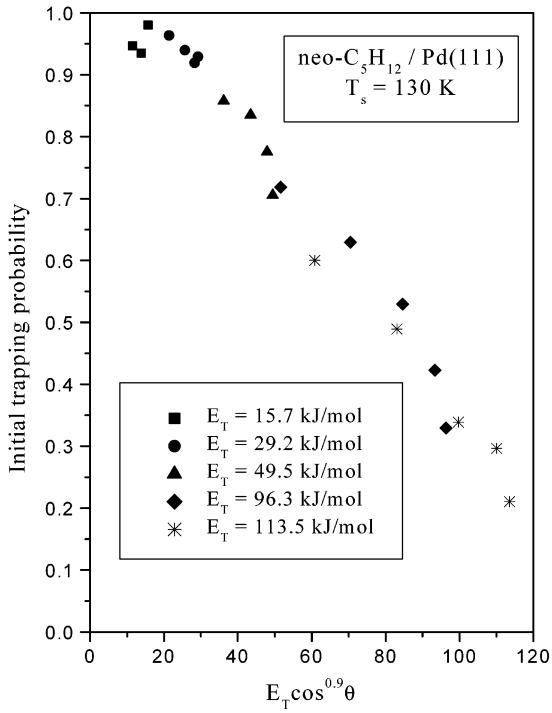

Figure 3. Initial trapping probability of neopentane on Pd(111) plotted as a function of $E_T \cos^{0.9}\theta$ at a surface temperature of 130 K. The incident angle is measured from the surface normal. The incident energies, E_T, are 15.7 (■), 29.2 (●), 49.5 (▲), 96.3 (♦), and 113.5 (*) kJ/mol, respectively.

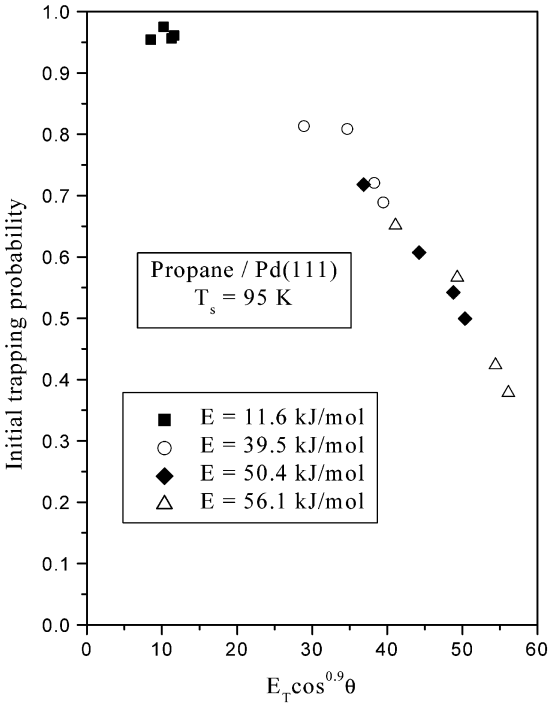

Figure 2. Initial trapping probability of propane on Pd(111) at the surface temperature of 95 K plotted as a function of $E_T \cos^{0.9}\theta$. The incident angle is measured from the surface normal. The incident energies, E_T, are 11.6 (■), 39.5 (○), 50.4 (♦), and 56.1 (△) kJ/mol, respectively.

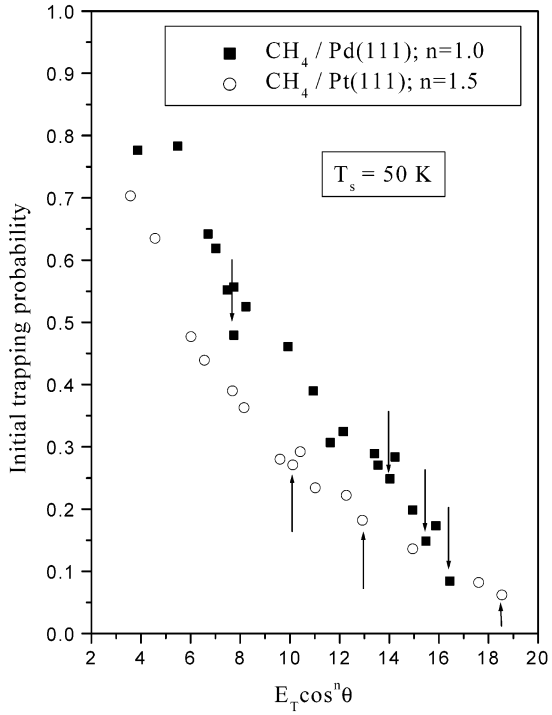

Figure 4. Comparison of the trapping probability of methane on Pd(111) and Pt(111) as a function of incident energy and angle. The energy functions for methane on palladium (■) and platinum (○) are $E_T \cos^{1.0}\theta$ and $E_T \cos^{1.5}\theta$, respectively. The experimental data on Pt(111) are from previous results. Points at normal incidence are marked with arrows.

4. Discussion

4.1. Mass Effect. The dependencies of the trapping probability of methane on the incident energy and angle on the Pd(111) and Pt(111) surfaces are compared in Figure 4. Points at normal incidence are marked with arrows. It is clear that the trapping probability of methane on Pd(111) is consistently higher than it is on Pt(111). A simple explanation is that methane molecules transfer more incident translational energy to the Pd surface rather than the Pt surface because of the lighter mass of the palladium, so that methane is more likely to trap on

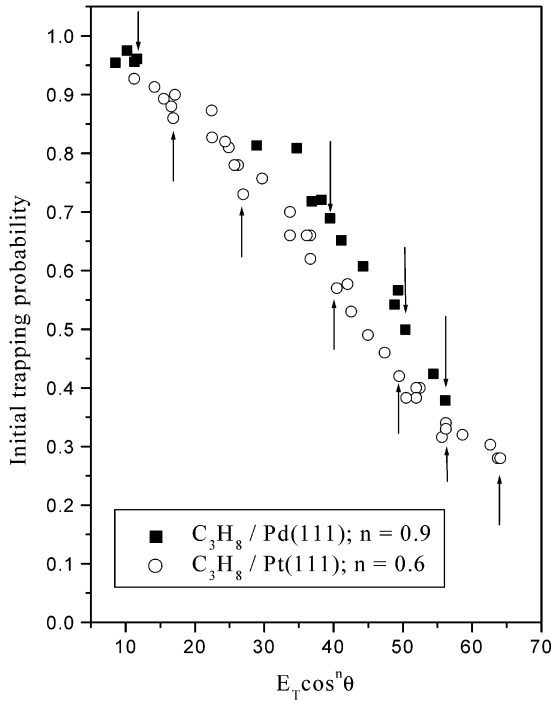

Figure 5. Comparison of the trapping probability of propane on Pd(111) and Pt(111) as a function of incident energy and angle. The energy functions for propane on palladium (■) and platinum (○) are $E_T\cos^{0.9}\theta$ and $E_T\cos^{0.6}\theta$, respectively. The experimental data for propane on Pt(111) are from previous results. Points at normal incidence are marked with arrows.

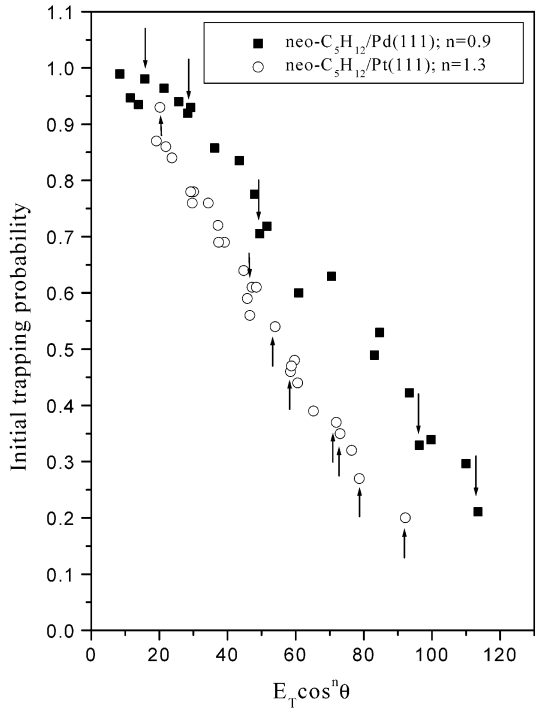

Figure 6. Comparison of the trapping probability of neopentane on Pd(111) and Pt(111) as a function of incident energy and angle. The energy functions for neopentane on palladium (■) and platinum (○) are $E_T\cos^{0.9}\theta$ and $E_T\cos^{1.3}\theta$, respectively. The experimental data for neopentane on Pt(111) are from previous results. Points at normal incidence are marked with arrows.

Pd(111). The modified Baule formula[19] gives the energy transfer in a collision as

$$\Delta = \frac{4\mu}{(\mu+1)^2}(E_T + D) \qquad (1)$$

where μ is the ratio of incident molecule mass to the surface atom mass, E_T is the incident molecule energy, and D is the well depth of a one-dimension square potential. Because the mass of palladium (mass = 106.4) is much less than that of platinum (mass = 195.09), the energy transfer is expected to be higher for methane trapping on Pd(111). Therefore, the trapping probability is expected to be higher on Pd(111), consistent with experiments. However, the Baule relationship fails to account quantitatively for the differences observed on the two surfaces. In addition, the trapping probability of methane scales $E_T\cos^{1.0\pm0.1}\theta$ on Pd(111), differing significantly from Pt(111) ($E_T\cos^{1.5\pm0.1}\theta$).[4] The energy scaling functions indicate a somewhat more corrugated gas−surface potential for the Pd(111).[11]

The dependencies of the trapping probabilities of propane and neopentane on Pd(111) and Pt(111)[18,29] on incident energy and angle are compared in Figures 5 and 6. Points at normal incidence are marked with arrows. The trapping probability of propane on Pd(111) is slightly higher than that on Pt(111), and within experimental error, the angular dependences on two different surfaces are identical. Like methane and propane, the initial trapping probability of neopentane on Pd(111) is higher than that on Pt(111). The energy scaling of neopentane on Pd(111) suggests a somewhat less corrugated gas−surface potential than for the Pt(111) surface. Overall, the differences observed for methane, propane, and neopentane trapping on Pd(111) and Pt(111) are qualitatively consistent with the different atomic mass of the surface atoms.

TABLE 2: Parameters for the Modified Kisliuk Model of Methane on Pd(111)

E_T (kJ/mol)	θ_i	S_0 (exp)	S_0 (model)	S_0' (exp)	S_0' (model)
7.7	0	0.497	0.497	0.89	1.00
15.5	45	0.390	0.390	0.86	0.97

4.2. Coverage Dependence. The adsorption probability is easily measured from the King and Wells trace as coverage accumulates on the surface. The adsorption behavior of methane on methane-covered Pd(111), on which the trapping probability increases with increasing coverage for all incident energies and incident angles, was successfully modeled by the modified Kisliuk model[1] (eq 2, Figure 7)

$$S(\theta) = S_0(1-\theta) + \frac{S_0'(1-\theta)q_m\theta}{1-q_m\theta} \qquad (2)$$

S_0 was determined from the King and Wells curve when the crystal is first exposed to the beam. S_0', was obtained from the King and Wells trace from the lowest partial pressure exhibited during the uptake, i.e., the value right before saturation. An alternative value for S_0' (model) was obtained by best fitting the coverage dependence of $S(\theta)$ according to eq 2. The parameters of the modified Kisliuk model for methane are summarized in Table 2. S_0' shows little dependence on either incident angle or energy over the range studied. The value of S_0' determined by eq 2 is higher than value determined from the lowest pressure in the King and Wells curve by 3∼15%. This difference has been discussed by Arumainayagam et al.[1] and been attributed to competitive desorption from the extrinsic precursor state, because the measurement was taken at a temperature at which the second layer is unstable.

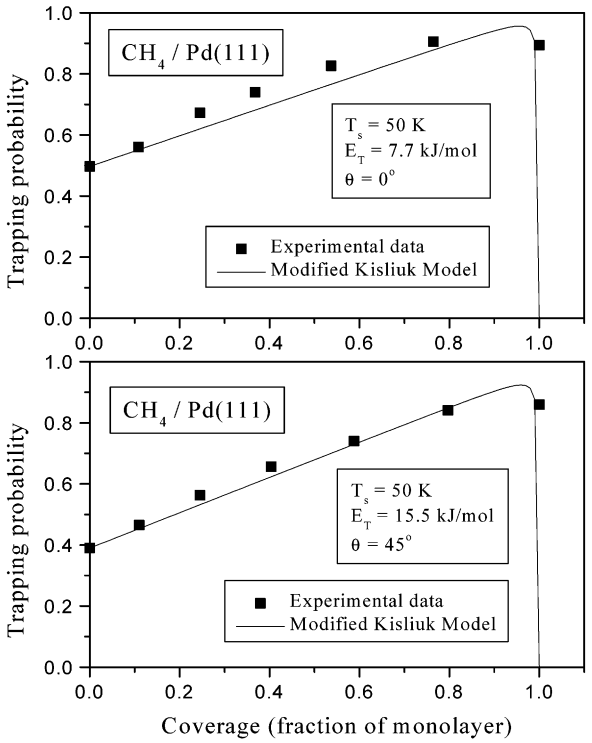

Figure 7. Coverage dependence of the methane adsorption probability with the incident energy of 7.7 kJ/mol at normal (top) and 15.5 kJ/mol at glancing (bottom) incidences. The solid squares indicate the experimental data and the solid lines indicate the results of the modified Kisliuk model.

TABLE 3: Parameters for the Modified Kisliuk Model of Propane on Pd(111)

E_T (kJ/mol)	θ_i	S_0 (exp)	S_0 (model)	S_0' (exp)	S_0' (model)
39.5	0	0.689	0.689	0.81	0.92
56.1	45	0.652	0.652	0.62	0.75

TABLE 4: Parameters for the Modified Kisliuk Model of Neopentane on Pd(111)

E_T (kJ/mol)	θ_i	S_0 (exp)	S_0 (model)	S_0' (exp)	S_0' (model)
29.2	0	0.929	0.929	0.95	0.98
113.5	30	0.339	0.339	0.73	0.81

The dependence of the trapping probability of propane and neopentane on Pd(111) on self-coverage depends on the angle of incidence. At angles of incidence of 0 and 30° the trapping probability increases with increasing coverage, as predicted by the modified Kisliuk model (Figures 8 and 9); adsorbed alkane layers facilitate its trapping. The trapping probability falls when the surface is close to saturated, most probably because the molecules desorbed before they find a binding site. The parameters of the modified Kisliuk model for propane and neopentane on Pd(111) are summarized in Tables 3 and 4.

4.3. General Comparison. The initial trapping probabilities of methane, ethane, propane, and neopentane on Pd(111) are plotted in Figure 10 against $E_T \cos^{1.0}\theta$. The slight scatter of the points on the curves of ethane, propane, and neopentane is due to the fact that $\cos^{1.0}\theta$ is not the best scaling for these alkanes, but a common scaling parameter was chosen to facilitate comparison. The trapping probability increases with molecular weight at a fixed incident energy on Pd(111).[18,29] This behavior is generally expected from simple classical mechanics because both the mass and the adsorption energies of the alkanes increase with their molecular weight (eq 1). Furthermore, the larger

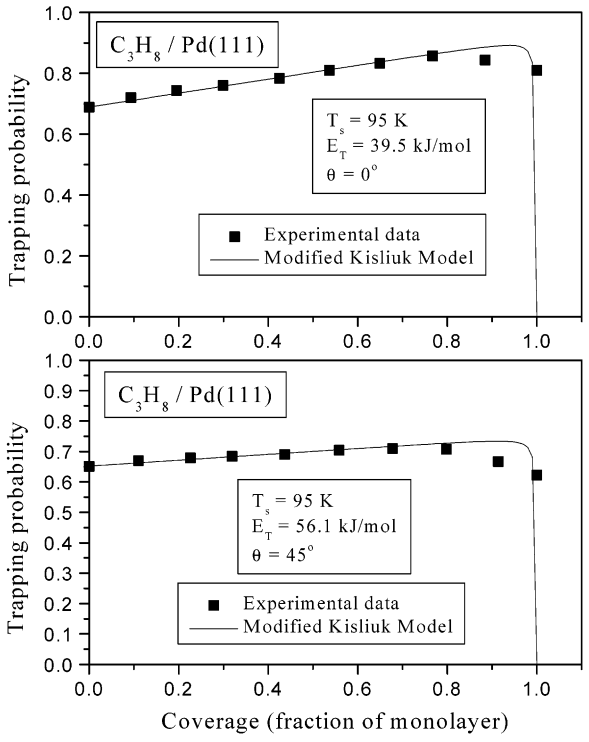

Figure 8. Coverage dependence of the propane adsorption probability with the incident energy of 39.5 kJ/mol at normal (top) and 56.1 kJ/mol at glancing (bottom) incidences. The solid squares indicate the experimental data and the solid lines indicate the results of the modified Kisliuk model.

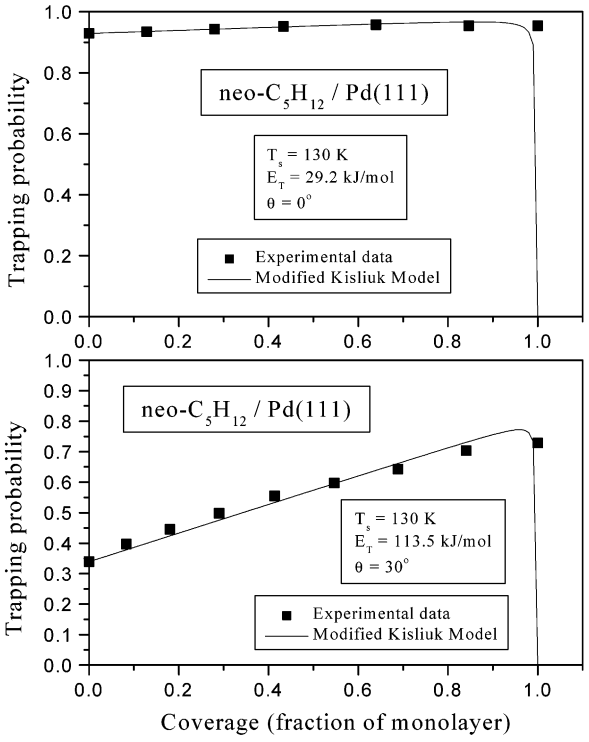

Figure 9. Coverage dependence of the neopentane adsorption probability with the incident energy of 29.2 kJ/mol at normal (top) and 113.5 kJ/mol at glancing (bottom) incidences. The solid squares indicate the experimental data and the solid lines indicate the results of the modified Kisliuk model.

alkanes have more complicated structures, opening more channels for transfer of energy from translation to internal modes of motion of the molecule. Last, the higher values of the trapping

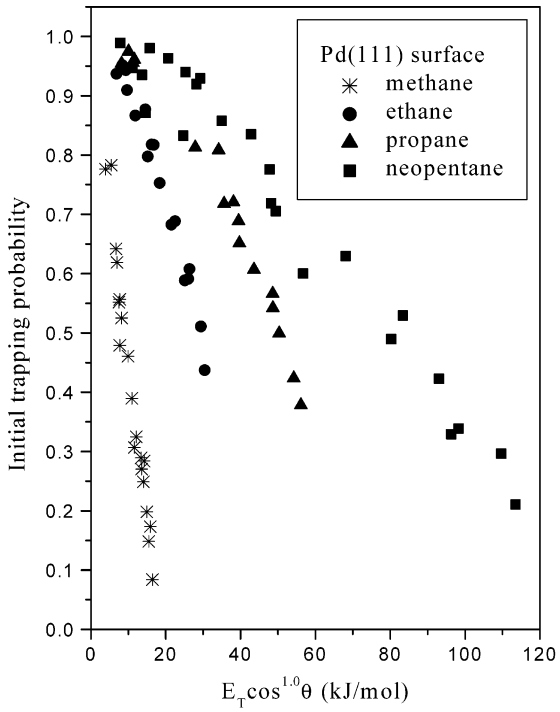

Figure 10. Initial trapping probability of methane (*), ethane (●), propane (▲), and neopentane (■) on Pd(111) plotted as a function of $E_T \cos^{1.0}\theta$. The incident angle is measured from the surface normal.

probability on Pd(111) are consistent with the lower mass of the palladium atom.

5. Simulations

Because the parameters that govern the interactions between the incident alkane and the Pt(111) and Pd(111) surfaces are so similar, the prediction of the trapping probabilities on Pd(111) from the two-body, central force methyl(methylene)−Pt derived from measurements of alkane trapping on Pt(111) appears feasible. Previous work has established that this potential, determined from measurements of ethane trapping on Pt(111), predicts the trapping probabilities of C_1-C_5 alkanes on Pt(111)[23,29] and C_2 and C_3 alkanes on Pt(110).[23] A successful prediction of the trapping probabilities on Pd(111) would be a first step toward scaling from one metal surface to another.

Our use of stochastic, three-dimensional classical dynamics for the simulation of molecular adsorption has been described in detail by Tully,[27,28] and the simulation methods are described elsewhere.[22] In this study, we present only the gas−surface potentials employed for alkane interacting with palladium surfaces, whose temperatures were set the same as in the experiments.

5.1. Pd−Pd Potential. The palladium atoms for the Pd(111) surface were allowed to vibrate about their equilibrium positions, which were taken to be the bulk-terminated positions. The palladium−palladium potential was represented by nearest neighbor (NN) and next nearest neighbor potential (NNN) harmonic force constants, which were scaled[14] from those we used in Pt(111).[22] The parameters used for Pd(111) were $k_{NN} = 32.8$ kg/s^2 and $k_{NNN} = 7.7$ kg/s^2. The friction constant applied to the bottom layer in the z direction was 2.19×10^{13} s^{-1}. These parameters successfully reproduce the bulk Debye temperature of palladium of 274 K[16] and the surface Debye temperature of 144 K.[10]

5.2. Alkane-Pd Potentials. Methane, propane, and neopentane were each modeled by the united atom methodology,[20,5] which represents each CH_n in an alkane molecule as a single interaction center. In other words, methane, propane, and neopentane were represented as pseudomonatomic, pseudotriatomic, and pseudopentaatomic, respectively. Identical Morse potential functions were taken for each of the CH_n constituents interacting with a single palladium atom. The Morse potential energy function is given by

$$V = \epsilon(\exp(-\sigma(r - r_0)) - 1)^2 - \epsilon(\exp(-\sigma(r_c - r_0)) - 1)^2, \quad r < r_c$$

$$V = 0, \quad r > r_c$$

where the three potential parameters are (i) the well depth ϵ, (ii) the position of the potential minimum r_0, and (iii) the range parameter σ. The cutoff distance, r_c, outside of which the potential was taken to be zero, was set to 9 Å. The distance r was taken to be the separation between a methyl group and surface atoms or cutoff distance, whichever is smaller. A sum of the interactions of each CH_n group with palladium atoms yields the total gas−surface potential.

Two sets of Morse potential parameters were used to describe the CH_n−Pd interaction in this study. The first set was taken, unadjusted, from the previous successful simulations of the dependence of the trapping probability of ethane on Pt(111) on incident energy and angle ($\epsilon = 2.53$ kJ/mol, $\sigma = 1.5$ Å^{-1}, $r_0 = 3.1$ Å), hereafter referred to as case A.[22] These parameters were determined from a single set of experiments-one molecule on Pt(111). These empirical potential parameters served as the basis for subsequent predictions, leading to accurate predictions of the trapping probabilities of propane on Pt(111) and Pt(110)[23] and predicting the absolute values of the trapping probabilities of *n*-butane, isobutene, and neopentane on Pt(111) to within a factor of 2.[29] This potential also predicts adsorption energies for methane, ethane, propane, and neopentane on Pd(111) that agree with experiments to within 15% (Table 5).

TABLE 5: Binding Energies of Alkanes on Pd(111) as Determined Experimentally Using TPD and Computed Using a Morse Potential with Parameters from Case A and Case B[a]

	experiment	case A	case B
methane	16.5	14.1	13.5
ethane	30.0	28.3	26.9
propane	41.5	42.1	39.8
neopentane	51.5	51.3	49.7

[a] Energies are given in kJ/mol.

Because this set of parameters did not exactly reproduce the trapping probabilities measured for the butanes and neopentane on Pt(111), they were adjusted to achieve a more accurate account of the trapping and scattering dynamics of all the alkanes on Pt(111).[29] These parameters ($\epsilon = 1.69$ kJ/mol, $\sigma = 1.15$ Å^{-1}, $r_0 = 3.1$ Å) are hereafter referred to as case B. This Morse potential also yields the desorption energies of alkane on Pd(111) to within experimental error (Table 5). The main difference between cases A and B is that the steepness of the repulsion is reduced in case B. The predictions resulting from simulations using each potential will be presented in detail in section 6.

5.3. Intramolecular Alkane Potentials. As mentioned above, the surface−alkane interaction was modeled according to the united atom approach in which the CH_n groups are represented as a single interaction center interacting with each of the metal atoms in the slab. Hence, propane was assumed to consist of two methyl groups each bound to a single methylene group. Neopentane was modeled to consist of four CH_3 groups each

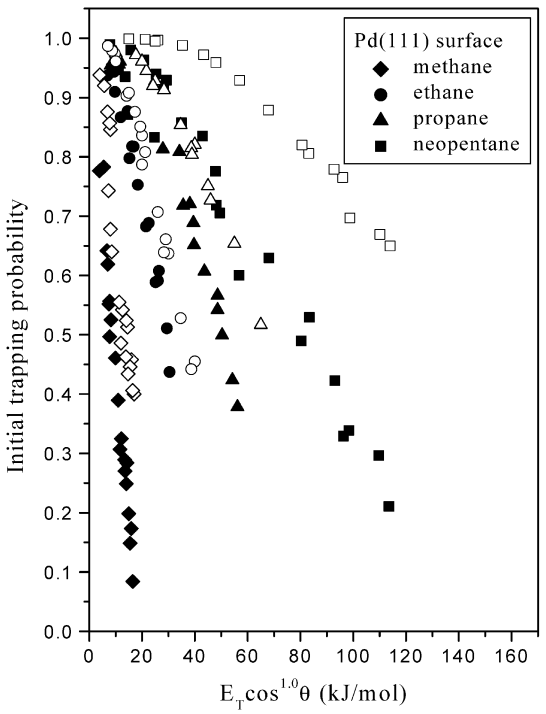

Figure 11. Initial trapping probabilities from experiments and simulation case A for methane (♦), ethane (●), propane (▲), and neopentane (■) trapping on Pd(111) plotted versus the function of $E_T \cos^{1.0}\theta$. Open symbols are for simulation results and solid symbols represent experimental data.

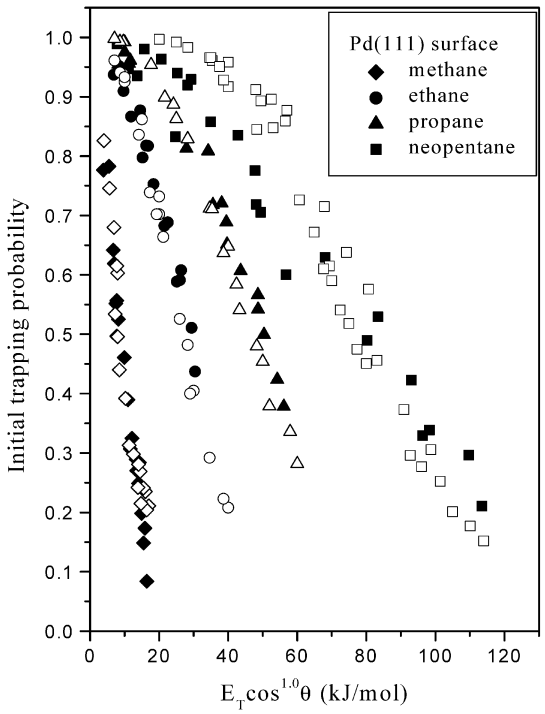

Figure 12. Initial trapping probabilities from experiments and simulation case B for methane (♦), ethane (●), propane (▲), and neopentane (■) trapping on Pd(111) plotted versus the function of $E_T \cos^{1.0}\theta$. Open symbols are for simulation results and solid symbols represent experimental data.

bound to the central carbon atom. The intramolecular interactions for propane and neopentane include C−C bond stretching and C−C−C bond angle bending. The applicable Morse parameters that account for C−C stretching were taken from previous work (ϵ = 347 kJ/mol, σ = 2.0 Å^{-1}, and r_0 = 1.7 Å).[22,23] The C−C−C bending force constant was taken to be 590 kJ/mol rad^2,[26] and the equilibrium C−C−C bond angles for propane and neopentane used were 112.4° and 109.5°, respectively.[26] Explicit inclusion of the hydrogen atoms of methane, propane, and neopentane was assumed to be unnecessary because of the high C−H stretching frequency (∼3000 cm^{-1}).[12]

6. Predictions of the Simulations

The calculated trapping probabilities for methane, ethane, propane, and neopentane on Pd(111) using potential parameters of case A are plotted against the scaling function of $E_T \cos^{1.0}\theta$ in Figure 11. The results for ethane trapping on Pd(111) were taken from previous work.[14] The simulations overestimate the trapping probabilities for all alkanes on Pd(111): the overestimation is particularly large for neopentane. Similar behavior was observed for the prediction for the trapping probability for neopentane on Pt(111) using this potential.[29] The overestimation of the initial trapping probabilities from case A suggests that either the amount of energy transferred to the surface is too large, and the steepness of potential repulsion (σ) should be reduced, or the well depth of attraction is too large, and ϵ should be reduced. On the other hand, simulations with case A predict the energy scaling exponent of alkanes to within experimental error (Table 6) except for methane. The agreement in energy scaling implies that the gas−surface *corrugation* is well represented by potential A.

Using the adjusted potential[29] (case B), a more accurate prediction of the trapping dynamics of alkanes on Pd(111) was achieved (Figure 12). It should be noted that potential B was obtained from experiments on Pt(111) only. For methane, the simulations reproduce the initial trapping probabilities up to the incident energy of 15 kJ/mol. For ethane and propane, the calculated initial trapping probabilities agree quite well with the measured values. For neopentane, the predictions are most accurate at high incident energies but slightly overestimate the magnitudes of the initial trapping probabilities by no more than 0.2 at low incident energies. Significantly, potential B also quantitatively reproduces the initial trapping probabilities of alkanes on Pt(111) (Figure 13), demonstrating for the first time that a single set of potential can predict the trapping probabilities of alkanes on *both* Pt(111) and Pd(111) *without* any adjustment. Additionally, the simulations with potential B also predict reasonably well the scaling exponents for the alkanes to within experimental error (Table 9). Overall, the main features of alkanes trapping on Pd(111) are well represented by potential B.

TABLE 6: Energy Scaling Exponent of Alkanes on Pd(111) as Determined Experimentally and Computed Using a Morse Potential with Parameters from Case A and Case B

	experiment	case A	case B
methane	1.0 ± 0.1	0.5 ± 0.1	0.7 ± 0.1
ethane	0.9 ± 0.1	0.85 ± 0.05	1.1 ± 0.1
propane	0.9 ± 0.1	1.0 ± 0.1	1.0 ± 0.1
neopentane	0.9 ± 0.1	0.8 ± 0.1	1.3 ± 0.1

7. Discussions

To better understand the energy transfer mechanism during the trapping of alkanes on Pd(111), the amount of energy partitioned into the various modes after the first bounce was averaged over 2000 trajectories, because simulations suggest that trapping is determined to within 5% by the fate of the first bounce of collisions. Thus, the energy profiles resulting from

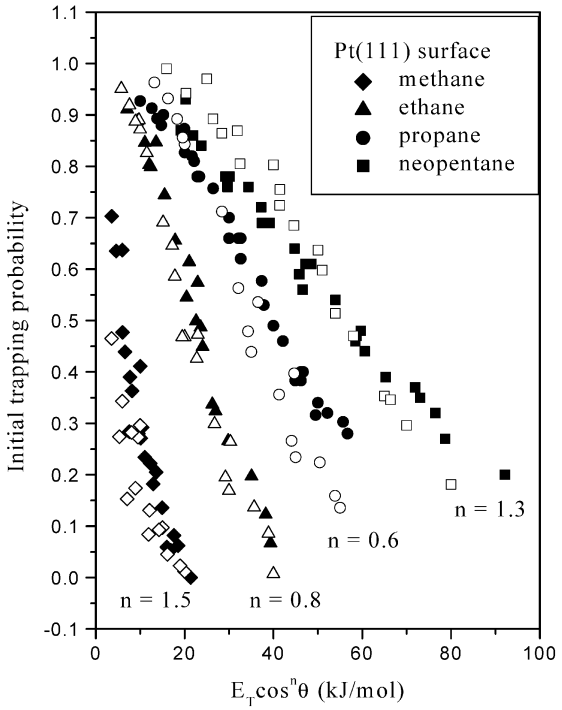

Figure 13. Initial trapping probabilities from experiments and simulation case B for methane (♦), ethane (▲), propane (●), and neopentane (■) trapping on Pt(111) plotted versus the function of $E_T \cos^n\theta$. The energy exponents, *n*, for methane, ethane, propane, and neopentane are 1.5, 0.8, 0.6, and 1.3, respectively. Open symbols are for simulation results and solid symbols represent experimental data.

the first bounce provide insight for understanding the energy transfer mechanism that governs the adsorption process. Of the energy modes available to the alkanes to dissipate incident energy during trapping, only including rotation, in-plane and perpendicular translation, vibration, and surface vibrations were considered important. The ethane molecules were treated as pseudodiatomic; hence, the two-dimensional rotation motion of ethane can be further decomposed into cartwheel and helicopter rotation. Excitation of the internal vibrations of ethane and propane was considered to be highly unlikely because the C−C stretch of ethane is about 1000 cm^{-1} and the characteristic time for vibration is much faster than the effective collision time of ethane with metal surfaces.[22]

Tables 7−10 enumerate the differences between the energy transferred into the respective modes for trapped and scattered methane, ethane, propane, and neopentane incident upon Pd(111). For methane trapping on Pd(111), both parallel energy and surface phonon excitation determine whether methane scatters after a single bounce or is trapped on the surface, except for higher energies at glancing incidence. Simulations also suggest that at glancing incidence, methane trapping is enhanced when trajectories gain parallel translational energy. This result is similar to that observed for methane trapping on Pt(111).[23] For all other molecules excitation of rotation and surface vibration contribute most to dissipation of the incident kinetic energy, enabling trapping.

Figure 14 illustrates the difference in the average energies resulting after the first bounce from ethane incident at Pd (111) with (a) 20 kJ/mol at 0° and (b) 40 kJ/mol at 45°. Even though the normal incident energies for those two cases are the same, the dominating factors for trapping are quite different. For ethane trapping on Pd(111) the excitation of lattice vibrations and cartwheel rotational excitation facilitating trapping, with the retention of parallel momentum playing a significant role at

TABLE 7: Table of Averages and Differences of Energy Storage Mechanisms Resulting after the First Bounce from Methane Incident at Pd (111) with 8 and 14.5 kJ/mol at 0° and 45° [a]

	temp. trapped	one bounce scat.	difference
Normal Incident, 8 kJ/mol (α = 0.656)			
parallel	3.3	1.1	2.2
perpendicular	−3.4	1.8	−5.1
phonon	8.1	5.2	2.9
Glancing Incident (45°), 8 kJ/mol (α = 0.772)			
parallel	4.6	2.0	2.6
perpendicular	−3.7	1.3	−4.9
phonon	7.1	4.7	2.3
Normal Incident, 14.5 kJ/mol (α = 0.313)			
parallel	5.6	2.1	3.4
perpendicular	−2.5	4.1	−6.6
phonon	11.4	8.2	3.1
Glancing Incident (45°), 14.5 kJ/mol (α = 0.407)			
parallel	9.1	4.1	5.0
perpendicular	−3.2	2.7	−5.9
phonon	8.6	7.7	0.9

[a] All energies are in kJ/mol. Columns labeled "one bounce scattered" and "temporarily trapped" represent the average energies of trajectories that scatter after a single bounce and those that experience at least a second bounce, respectively. The column labeled "difference" represents the difference between these energies.

TABLE 8: Table of Averages and Differences of Energy Storage Mechanisms Resulting after the First Bounce from Ethane Incident at Pd (111) with 20 and 40 kJ/mol at 0° and 45° [a]

	temp. trapped	one bounce scat.	difference
Normal Incident, 20 kJ/mol (α = 0.702)			
cartwheel	4.0	1.9	2.1
helicopter	1.4	0.9	0.5
parallel	3.0	2.4	0.6
perpendicular	−6.1	3.4	−9.5
phonon	17.7	11.5	6.2
Glancing Incident (45°), 20 kJ/mol (α = 0.836)			
cartwheel	5.3	1.9	3.4
helicopter	1.1	1.0	0.1
parallel	7.5	4.5	3.0
perpendicular	−8.3	2.7	−11.0
phonon	14.3	10.0	4.4
Normal Incident, 40 kJ/mol (α = 0.208)			
cartwheel	7.7	2.8	4.9
helicopter	2.6	1.7	0.9
parallel	4.3	3.4	1.0
perpendicular	−4.4	8.5	−12.9
phonon	29.8	23.6	6.1
Glancing Incident (45°), 40 kJ/mol (α = 0.482)			
cartwheel	9.1	3.2	5.9
helicopter	1.7	1.9	−0.1
parallel	14.5	10.6	3.9
perpendicular	−6.2	5.1	−11.4
phonon	20.9	19.3	1.6

[a] All energies are in kJ/mol.

higher angles of incidence. The relative importance of cartwheel rotational excitation in determining trapping is less at lower initial translational energy, especially at normal incidence. This finding is slightly different from the results for ethane trapping on Pt(111),[22] for which the cartwheel rotational excitation of ethane during the first bounce is the most important mechanism that distinguishes trapping from scattering.

For propane trapping on Pd(111), at normal incidence, rotational excitation assists trapping, but the excitation of surface phonons dominates the adsorption process. At glancing incidence, the importance of retention of parallel momentum

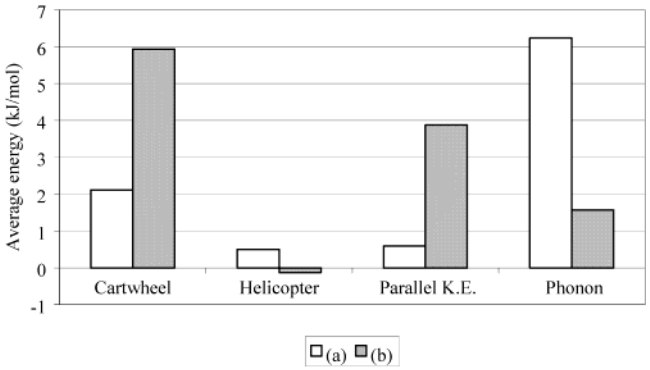

Figure 14. Difference of average energies resulting after the first bounce from ethane incident at Pd (111) with (a) 20 kJ/mol at 0° and (b) 40 kJ/mol at 45°. Histograms for cartwheel rotational, helicopter rotational, parallel translational, and surface phonon energies are shown.

TABLE 9: Table of Averages and Differences of Energy Storage Mechanisms Resulting after the First Bounce from Propane Incident at Pd(111) with 40 and 60 kJ/mol at 0° and 45° [a]

	temp. trapped	one bounce scat.	difference
Normal Incident, 40 kJ/mol ($\alpha = 0.648$)			
rotation	9.1	5.8	3.3
parallel	4.1	3.1	1.0
perpendicular	−7.5	6.2	−13.6
phonon	34.1	24.7	9.4
Glancing Incident (45°), 40 kJ/mol ($\alpha = 0.829$)			
rotation	10.2	5.8	4.4
parallel	13.5	9.4	4.1
perpendicular	−10.3	3.8	−14.1
phonon	26.4	20.8	5.6
Normal Incident, 60 kJ/mol ($\alpha = 0.282$)			
rotation	12.4	7.7	4.7
parallel	4.8	4.1	0.7
perpendicular	−4.7	10.2	−14.9
phonon	47.2	37.6	9.6
Glancing Incident (45°), 60 kJ/mol ($\alpha = 0.584$)			
rotation	13.1	7.7	5.4
parallel	20.5	15.3	5.2
perpendicular	−7.3	5.5	−12.8
phonon	33.8	30.5	3.3

[a] All energies are in kJ/mol.

TABLE 10: Table of Averages and Differences of Energy Storage Mechanisms Resulting after the First Bounce from Neopentane Incident at Pd (111) with 114 kJ/mol at 0° and 45° [a]

	temp. trapped	one bounce scat.	difference
Normal Incident, 114 kJ/mol ($\alpha = 0.152$)			
rotation	15.2	9.7	5.5
vibration	6.3	3.6	2.6
parallel	8.4	3.9	4.5
phonon	92.6	73.2	19.4
Glancing Incident (45°), 114 kJ/mol ($\alpha = 0.576$)			
rotation	19.5	12.7	6.8
vibration	4.7	4.3	0.4
parallel	31.1	19.5	11.7
phonon	69.7	63.4	6.2

[a] All energies are in kJ/mol.

increases, but both rotational excitation and surface phonons still positively contribute to the trapping of propane after the first bounce. The energy exchange processes which dictate trapping on Pd(111) differ from those for Pt(111), on which rotational excitation is the most important energy storage mechanism for trapping.[23]

For neopentane on Pd(111), at normal incidence, energy transfer to lattice phonons on the first bounce is the dominant process involved in trapping. At glancing incident angles, the relative importance of phonon excitation on determining trapping decreases, and the relative importance of rotational excitation and retention of parallel momentum increase. This finding is slightly dissimilar to neopentane trapping on Pt(111), in which, though surface phonons assist trapping, rotational excitation and retention of parallel momentum are the most effective energy storage mechanisms that distinguish trapping from scattering.[29] The primary reason for these differences must be the lower mass of palladium.

8. Conclusion

For the molecular adsorption of methane, propane, and neopentane on Pd(111), the scaling function for the initial trapping probabilities suggests that the gas−surface interaction potentials are significantly corrugated. In general, the trapping of alkane on Pd(111) increases with increasing coverage in the range of energies studied. The modified Kisliuk model successfully describes this coverage dependence. The trapping probability for each alkane is higher on Pd(111) than on Pt(111), consistent with the lower mass of the palladium atom.

The trapping probabilities of the alkanes were accurately *predicted* from the methyl(methylene)−Pt Morse potential obtained from alkanes trapping on *Pt*(111). Calculations of the energy transfer channels for alkanes trapping on Pd(111) indicate that the excitation of lattice phonons plays a more important role in trapping than on Pt(111); this result appears to originate from the lower mass ratio of the palladium atoms.

Acknowledgment. We would like to acknowledge the Department of Energy, Chemical Sciences Division, Office of Basic Energy Sciences (Grant No. DE-FG03-86ER13468-A016) for financial support of this work.

References and Notes

(1) Arumainayagam, C. R.; McMaster, M. C.; Madix, R. J. *J. Phys. Chem.* **1991**, *95*, 2461.
(2) Arumainayagam, C. R.; McMaster, M. C.; Schoofs, G. R.; Madix, R. J. *Surf. Sci.* **1989**, *222*, 213.
(3) Arumainayagam, C. R.; Schoofs, G. R.; McMaster, M. C.; Madix, R. J. *J. Phys. Chem.* **1991**, *95*, 1041.
(4) Carlsson, A. F.; Madix, R. J. *Surf. Sci.* **2000**, *458*, 91−105.
(5) Catlow, C. R. A.; Parker, S. C.; Allen, M. P. *Computer Modeling of Fluids, Polymers and Solids*; Kluwer Academic: London, 1990.
(6) D'Evelyn, M. P.; Hamza, A. V.; Gdowski, G. E.; Madix, R. J. *Surf. Sci.* **1986**, *167*, 451.
(7) D'Evelyn, M. P.; Steinruck, H. P.; Madix, R. J. *Surf. Sci.* **1987**, *180*, 47.
(8) Feulner, P.; Menzel, D. J. *J. Vacuum Sci. Technol.* **1980**, *17*, 662.
(9) Feulner, P.; Menzel, D. J. *Surf. Sci.* **1985**, *154*, 465.
(10) Goodman, R. M.; Farrell, H. H.; Somorjai, G. A. *J. Chem. Phys.* **1968**, *48*, 1046.
(11) Head-Gordon, M.; Tully, J. C. *Surf. Sci.* **1992**, *268*, 113.
(12) Herzberg, G. *Infrared and Raman Spectra*; Van Nostrand: New York, 1945.
(13) Kao, C.-L.; Carlsson, A. F.; Madix, R. J. *Top. Catal.* **2001**, *14*, 63.
(14) Kao, C.-L.; Weaver, J. F.; Madix, R. J. to be published **2002**.
(15) King, D. A.; Wells, M. G. *Surf. Sci.* **1972**, *29*, 454.
(16) Kittel, C. *Introduction to Solid State Physics*, 6th ed.; Wiley: New York, 1986.
(17) Lide, D. R. *CRC Handbook of Chemistry and Physics*, 81st ed.; CRC Press: Boca Raton, FL, 2001.
(18) McMaster, M. C.; Arumainayagam, C. R.; Madix, R. J. *Chem. Phys.* **1993**, *177*, 461.
(19) Persson, M.; Harris, J. *Surf. Sci.* **1987**, *187*, 67.
(20) Ryckaert, J. P.; Bellemans, A. *Faraday Discuss. Chem. Soc.* **1978**, *66*, 95.
(21) Schoofs, G. R.; Arumainayagam, C. R.; Madix, R. J. *J. Vaccum Sci. Technol. A* **1988**, *6*, 882.

(22) Stinnett, J. A.; Madix, J.; Tully, J. C. *J. Chem. Phys.* **1996**, *104*, 3134.
(23) Stinnett, J. A.; Madix, R. J. *J. Chem. Phys.* **1996**, *105*, 1609.
(24) Stinnett, J. A.; McMaster, M. C.; Schroeder, S. L. M.; Madix, R. J. *Surf. Sci.* **1996**, *365*, 683.
(25) Stinnett, J. A.; Weaver, J. F.; Madix, R. J. *Surf. Sci.* **1998**, *395*, 148.
(26) Sverdlov, L. M.; Kovner, M. A.; Krainov, E. P. *Vibrational Spectra of Polyatomic Molecules*; Wiley: New York, 1957.
(27) Tully, J. C. *Acc. Chem. Res.* **1981**, *14*, 188.
(28) Tully, J. C. In *Many Body Phenomenon at Surfaces*; Langreth, D., Suhl, H., Eds.; Academic: New York, 1984; pp 377−401.
(29) Weaver, J. F.; Madix, R. J. *J. Chem. Phys.* **1999**, *110*, 10585.